Int. Journal of Refractory Metals and Hard Materials 28 (2010) 669–673

Contents lists available at ScienceDirect

Int. Journal of Refractory Metals and Hard Materials

journal homepage: www.elsevier.com/locate/IJRMHM

Fracture toughness and microstructural characterization of polycrystalline rolled tungsten

D. Rupp [a,*], R. Mönig [a], P. Gruber [b], S.M. Weygand [c]

[a] Forschungszentrum Karlsruhe, Institute for Material Research II, Herrmann-von-Helmholtz-Platz 1, D-76344 Eggenstein-Leopoldshafen, Germany
[b] University of Karlsruhe, Institute for Reliability of Components and Systems, Kaiserstrasse 12, D-76131 Karlsruhe, Germany
[c] Karlsruhe University of Applied Sciences, Department of Mechanical Engineering and Mechatronics, Moltkestrasse 30, D-76133 Karlsruhe, Germany

ARTICLE INFO

Article history:
Received 14 December 2009
Accepted 8 May 2010

Keywords:
Tungsten
Fracture toughness
Brittle-to-ductile transition
In situ fracture test

ABSTRACT

Various fracture tests have been performed to determine the fracture toughness of sintered and rolled tungsten rods. The polycrystalline rods experienced a degree of deformation of about 65% after sintering and exhibited a pronounced fiber texture. Specimens with three different kinds of crack orientation were extracted and tested in the temperature range between −150 °C and 950 C. The results confirm the strong influence of the anisotropic microstructure on the fracture behavior and on the brittle-to-ductile transition. To gain insight into the failure mechanisms, a close analysis of the microstructure was done by scanning electron microscopy and electron backscatter diffraction. Furthermore, in situ experiments were conducted at elevated temperatures in the transition regime to study crack initiation and fracture. Auger spectroscopy showed segregations of phosphorus and fluorine at intergranular fracture surfaces.

1. Introduction

Body centered metals like tungsten generally fail brittle at lower temperatures and show a distinct transition from brittle-to-ductile fracture behavior with increasing temperature. The inherent brittleness and the relatively high transition temperature of tungsten are crucial issues with regard to many technological applications. A current field of research is for instance the application of tungsten and tungsten alloys as a plasma facing material in highly loaded components of future fusion power plants like the divertor [1].

The fracture toughness and the brittle–ductile transition (BDT) has been studied extensively for single crystalline tungsten [2,3], while data of polycrystalline tungsten are still rare. The transition temperature is not a material constant but depends strongly on parameters like loading rate, the fabrication route and impurities. Particularly for brittle metals, the microstructure plays a decisive role for the fracture process and the resulting fracture toughness. Thus, a detailed understanding of the fracture mechanisms, the controlling factors of the BDT and their interaction with the microstructure is essential to identify ways of improving these properties.

Polycrystalline tungsten is usually produced by a powder metallurgical route and is commercially available in many forms. The variation in the experimental data of previously published works [4–6] concerning the fracture toughness and the brittle-to-ductile transition (BDT) of polycrystalline tungsten and tungsten alloys emphasizes the strong influence of the production process and hence the microstructure. In this work, we focus on a very common variety, namely sintered and rolled tungsten rods, which show a pronounced fiber texture. In this textured system, specimens with different crack orientations have been used to study the influence of the microstructure on the fracture behavior of polycrystalline tungsten.

2. Experimental

The fracture toughness and the BDT of pure (99.98%) tungsten rods supplied by Plansee Metall GmbH, Reutte, Austria has been investigated. The rods experienced a break down rolling after sintering with a degree of deformation of 65% resulting in a diameter of 14 mm. Optical micrographs showed that the microstructure exhibited elongated grains with an aspect ratio of roughly 3:1 in the rolling direction. Furthermore, a close analysis of the microstructure was done by means of electron backscatter diffraction (EBSD). Selected specimens were polished for this purpose with a succession of diamond pastes. A final polishing step was done using SiO_2-suspension.

Our fracture mechanical tests were conducted on notched rectangular bars (3 mm×6 mm×27 mm) in three-point bending (25 mm span width) over the temperature range −150 °C−950 °C at a fixed loading rate of 1 μm/s. The fracture tests were performed in high vacuum for temperatures above 350 °C to avoid any oxidation of the specimens and in a cooling nitrogen atmosphere below room temperature. Specimens were fabricated by electrical discharge machining with 3 mm deep notches. Sharper crack starter notches were introduced by using a razor blade at the root of these first notches. Final notch depths and radii were typically 3.2 mm and 20 μm, respectively.

* Corresponding author.
E-mail address: daniel.rupp@kit.edu (D. Rupp).

0263-4368/$ – see front matter © 2010 Elsevier Ltd. All rights reserved.
doi:10.1016/j.ijrmhm.2010.05.006

To account for the anisotropic microstructure three specimen types with different kinds of crack orientations were investigated (see Fig. 1). As the transverse specimens (type I and II) are limited in their size, they were brazed to two extension arms to obtain the desired geometry.

To gain insight into the crack initiation and propagation process, in situ SEM fracture tests were performed using the same specimen sizes and geometry of the bending setup as for the conventional fracture tests. A tensile-compressive testing apparatus from Kammrath and Weiss was modified to perform three-point bending tests by exchanging the sample clamps to home built clamps for bending. For experiments at elevated temperatures, a small resistance heating system was attached underneath the specimens and the specimen temperature was measured in close vicinity to the notch root by a type K thermocouple. After mounting the samples and attaching the heater, the system was inserted into a Leo 1530VP scanning electron microscope. Stable imaging and operation of the whole setup could be achieved for temperatures as high as 500 °C. In the work presented here, we will focus on the type III specimen tested at 350 °C.

Intergranular fracture of tungsten has been attributed to the presence of impurities at grain boundaries such as phosphorus [7]; the nature and extent of impurities depend on the production process. Fracture surfaces were examined by Auger electron spectroscopy (AES) to study the impurity segregation at the grain boundaries. The Auger spectrometer used in this work was equipped with an in situ fracture apparatus so that specimens could be fractured in ultra high vacuum inside the specimen chamber.

3. Results and discussion

3.1. Microstructure

EBSD analysis of the microstructure showed that a <110> fiber texture has formed during rolling, which is particularly pronounced in the center of rods from where the specimens were extracted. Furthermore, a subgrain structure has formed as shown in Fig. 2, where the high (>15°) and low angle (between 2° and 15°) boundaries are plotted by lines of different grey levels. This finding was confirmed by transmission electron microscopy (TEM).

3.2. Fracture toughness and fractography

Fig. 3a shows the fracture toughness as a function of temperature for the investigated kinds of crack orientation. All three specimen types failed by brittle fracture at low temperatures and exhibited a transition from brittle-to-ductile fracture behavior with increasing temperature marked by a rapid increase in fracture toughness. As K_{IC} loses validity with increasing ductile behavior, the calculated values above the transition regime give only a lower bound and are denoted by open symbols. The results demonstrate that the anisotropic microstructure has a strong influence on the absolute values of fracture toughness as well as on the transition temperature. Most notably the type III specimens showed higher fracture toughness in the brittle regime and the brittle-to-ductile transition occurred at lower temperatures compared to the two transverse types. SEM investigations of the fracture surfaces revealed that the type I and II specimens failed predominately by intergranular fracture while the type III specimens exhibited almost exclusively transgranular cleavage surfaces in the brittle regime. No significant change of the fracture behavior and morphology could be observed for the two transverse types with increasing temperature; first dimple patterns appeared locally at 800 °C. In the transition range, the fracture behavior of type III specimens changed drastically, as shown in Fig. 3b. With increasing temperature the specimens did not fail catastrophically anymore but in a stepwise or stable manner. As can be seen from the load–displacement curve in Fig. 3b a distinct load drop could be observed at 275 °C followed by stable crack growth. Similar fracture behavior was found for higher temperatures with the exception that the load drops occurred after some plastic yielding; the load drops on the load–displacement curves were accompanied by audible clicks.

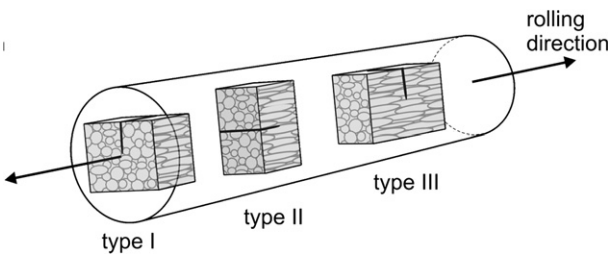

Fig. 1. Schematic representation of the investigated specimen types and crack orientations: in the first case the crack front is parallel (type I), in the second one radial (type II) and in the third case tangential (type III) to the rolling direction.

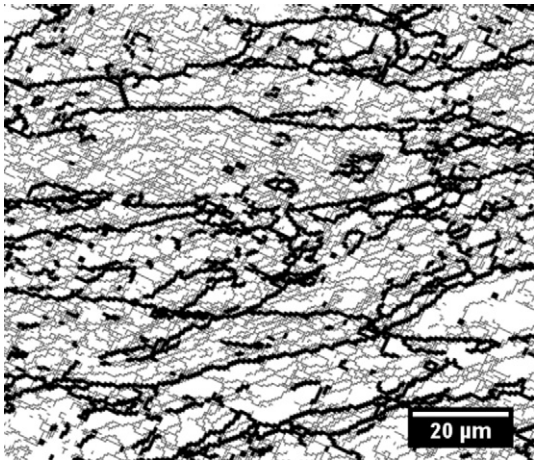

Fig. 2. High and low angle boundary distribution mapped by EBSD. Data were taken from a cross section parallel to the rolling direction. High angle boundaries with a misorientation above 15° are plotted in black and the lighter lines are the low angle boundaries between 2° and 15°.

Examination of the fractured specimens indicated that the load drop and the following stable crack growth can be associated with the initiation and growth of a symmetrically branched crack (see Fig. 4a). The branched crack grew primarily along the elongated grain boundaries in the rolling direction, while the material in the vicinity of the notch root failed by ductile fracture in a fibrous manner (Fig. 4b–d).

3.3. In situ 3 point bending

In situ fracture tests were performed in SEM to clarify the observed fracture behavior, particularly for the type III specimens in the transition regime. Snapshots of the experiment conducted on a type III specimen are shown in Fig. 5a–c to address the issue of crack branching. The specimen was heated up to about 350 °C and slowly loaded to fracture in displacement control. The load–displacement curve was recorded by the control of the stage and images from the notch tip region were continuously taken during the experiment..As can be seen from Fig. 5a, the first crack, which was accompanied with a distinct load drop in the load–displacement curve, was initiated in front of the notch. Most notably the crack was not oriented along the symmetry plane of the specimen but perpendicular to it, which corresponds to the rolling direction of the material. With increasing load the crack propagated in both directions and the remaining ligament between the notch root and the transverse crack finally

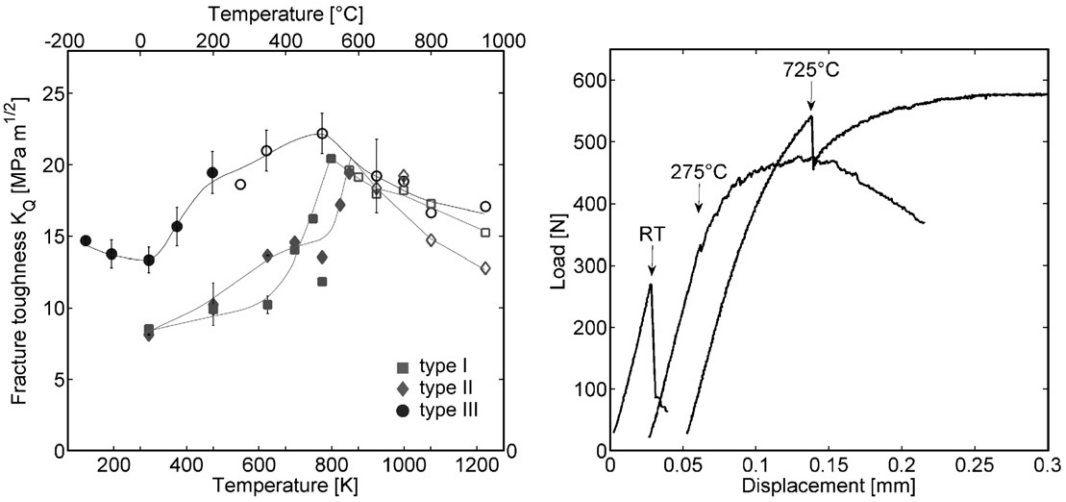

Fig. 3. a) Fracture toughness as a function of temperature for the three different crack orientations. Values in the region where linear fracture mechanics is no longer valid are denoted by the open symbols. b) Selected load–displacement curves of type III specimens. Curves are shifted for better visualization.

failed by shear fracture. EBSD measurements before and after the in situ experiment showed that the high angle grain boundaries in the rolling direction were the preferred crack paths (see Fig. 5d and e). The experimental results suggest that the observed change in the fracture behavior can be explained by the fact that crack propagation along the elongated grain boundaries in the rolling direction becomes favorable with increasing temperature.

3.4. Auger spectroscopy

First Auger measurements performed on the fracture surface of a type II specimen (see Fig. 5a) revealed that phosphorus and fluorine is present, but both elements are not uniformly distributed as shown in the corresponding element maps (see Fig. 6b and c). Further analyses indicated that both impurities are concentrated in the remaining

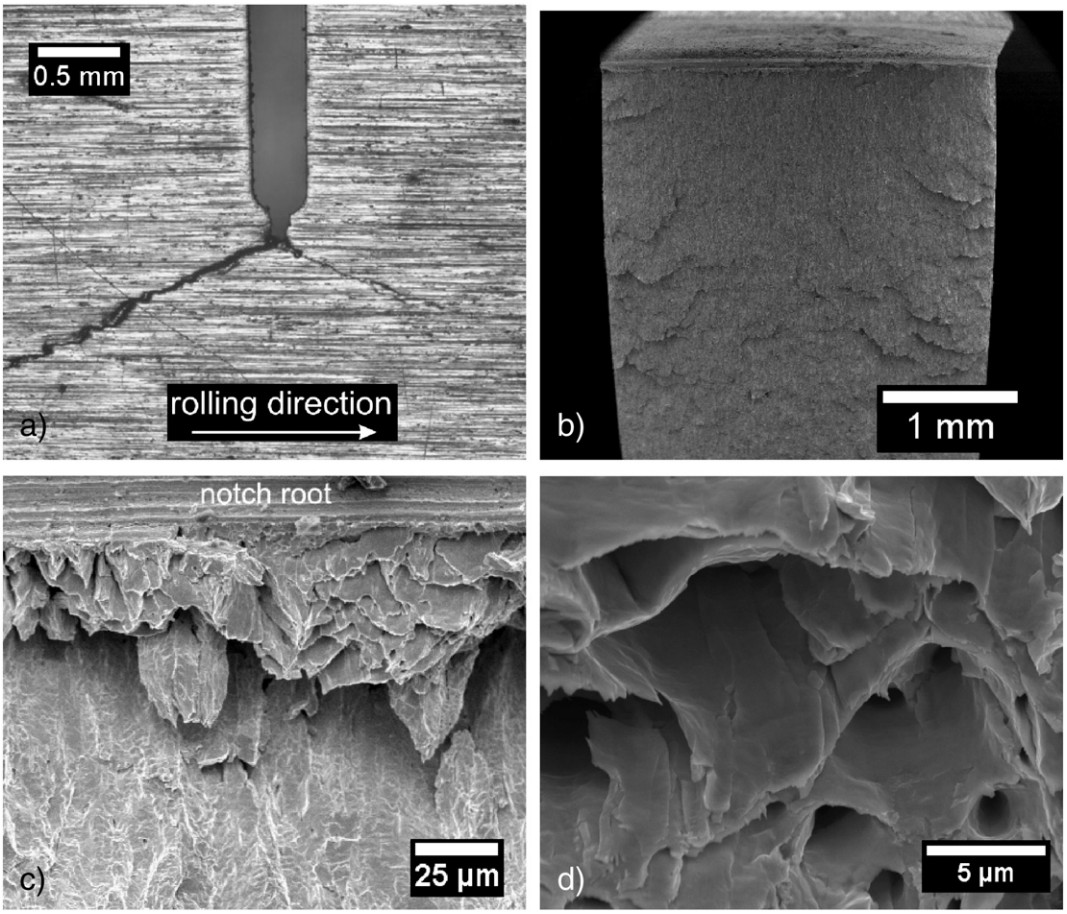

Fig. 4. a) Type III specimen tested in the transition regime at 275 °C showing crack branching. b) Specimen tested at 350 °C Top view on the fracture surface of one of the symmetrical crack branches such as shown in a). Figure c) shows the fibrous fracture pattern which was typically observed in close vicinity to the notch root. This area is marked by the white box in the top view of figure b). d) Image at higher magnification.

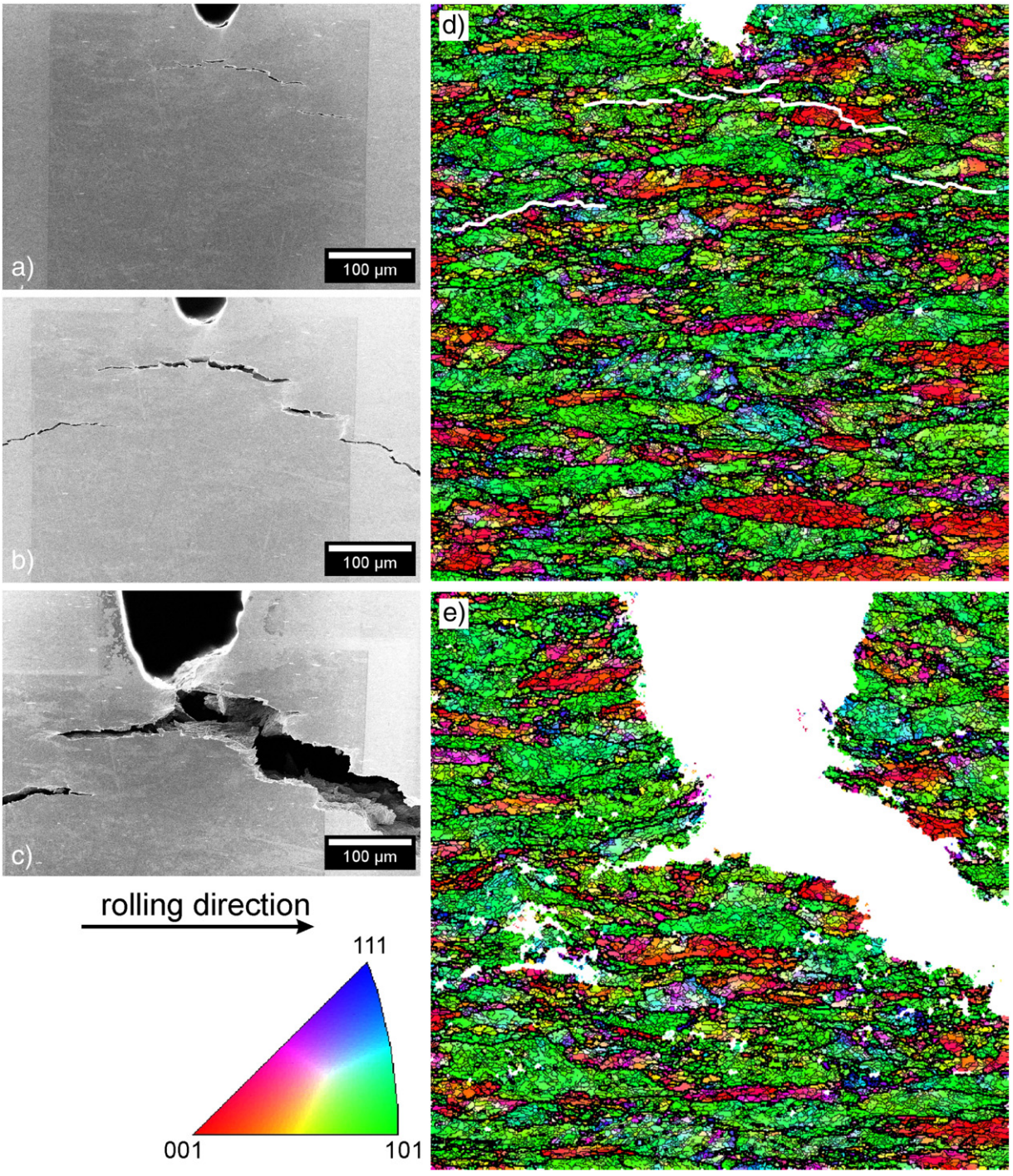

Fig. 5. In situ fracture test conducted on a type III specimen at 350 °C. Images of the notch tip region were taken continuously. Snapshots a)–c) showing the crack initiation and propagation with increasing applied load. EBSD orientation maps obtained from the notch tip region d) before and e) after the in situ experiment. Crystal orientation is given with respect to the rolling direction. Additionally, high (thick lines and low angle (thin lines) boundaries are plotted in the orientation map. The observed crack path can be linked to the microstructure by combining in situ observations with EBSD data, as shown in figure d) where the crack path is marked by the white lines.

sinter pores at the grain boundaries, which are also elongated in the rolling direction. Neither phosphorus nor fluorine could be detected in the Auger spectra taken from cleavage surfaces or "regular" grain boundaries.

4. Summary

The fracture toughness of sintered and rolled tungsten was investigated as function of temperature for different kinds of crack orientations with respect to the rolling direction. We found a strong influence of the microstructure on the fracture behavior and toughness as well as on the brittle-to-ductile transition temperature. The transverse specimens (type I and II in Fig. 1) with their crack front parallel or radial to the rolling direction failed primarily in an intergranular manner and showed much lower fracture toughness than the specimens oriented in the rolling direction (type III). The latter specimen type failed by transcrystalline cleavage at low temperatures and showed a distinct change in its fracture behavior in the transition regime. In situ fracture tests were performed in a scanning electron microscope to study the crack initiation and

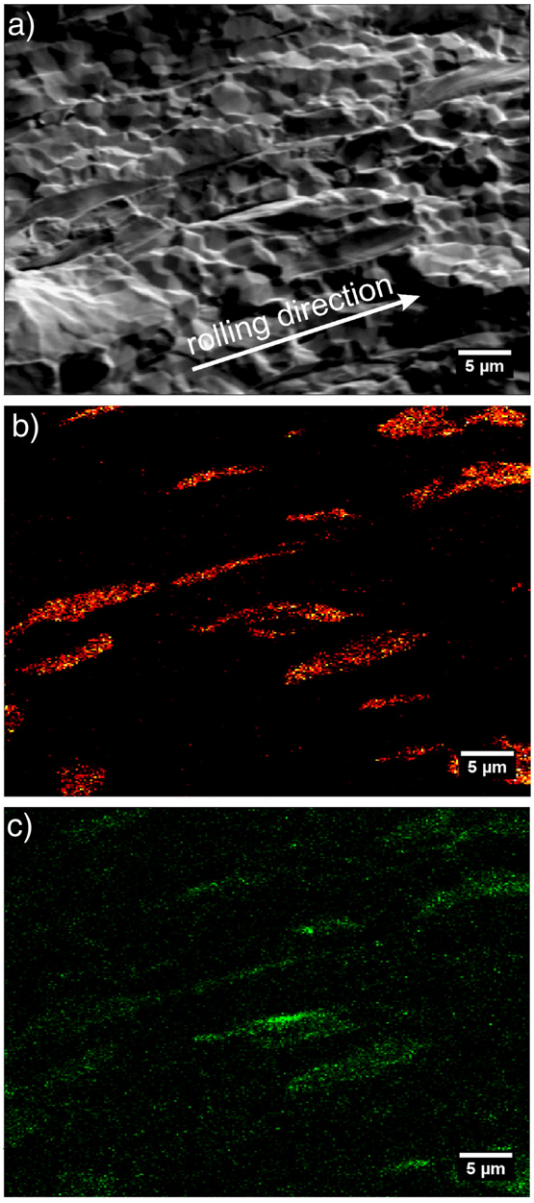

Fig. 6. a) SEM image of the investigated fracture surface showing primarily intergranular fracture. b) Phosphorus and c) fluorine distribution on the fracture surface obtained by AES. Brighter areas have a higher concentration of the element.

propagation process showing that the first crack is initiated in front of the notch tip in the rolling direction. By using the combined technique of in situ fracture tests and electron backscatter diffraction, the crack origin and path could be linked to the microstructure. The experimental results suggest that the elongated grain boundaries parallel to the rolling direction play a decisive role in the fracture process for all crack orientations, as they are the preferred crack paths (type I and II) or become favorable with increasing temperature (type III). Auger spectroscopy measurements revealed phosphorus and fluorine at these intergranular fracture surfaces.

Acknowledgements

The authors wish to thank Eberhard Nold of IMF I, Forschungszentrum Karlsruhe for carrying out the Auger measurements. They acknowledge the Max-Planck-Institute Stuttgart for providing the in situ SEM equipment and Plansee Metall GmbH for supplying the tungsten material. The research was supported by the German Science Foundation DFG under Grant No. WE 4256/3-2 and the Research and Development Nuclear Fusion Programme of the Forschungszentrum Karlsruhe.

References

[1] Norajitra P, Abdel-Khalik SI, Giancarli LM, Ihli T, Janeschitz G, Malang S, et al. Divertor conceptual designs for a fusion power plant. Fusion Eng Des 2008;83:893–902.
[2] Riedle J. Der Bruchwiderstand in Wolfram-Einkristallen: Einfluss der kristallographischen Orientierung, der Temperatur und der Lastrate. VDI-Verlag: Düsseldorf; 1995 (in german).
[3] Gumbsch P, Riedle J, Hartmaier A, Fischmeister HF. Controlling factors for the brittle-to-ductile transition in tungsten single crystals. Science 1998;282:1293–5.
[4] Giannattasio A, Roberts SG. Strain-rate dependence of the brittle-to-ductile transition temperature in tungsten. Phil Mag A 2007;87:2589–98.
[5] Faleschini M, Kreuzer H, Kiener D, Pippan R. Fracture toughness investigations of tungsten alloys and SPD tungsten alloys. J Nucl Mater 2007;367–370:800–5.
[6] Margevicius RW, Riedle J, Gumbsch P. Fracture toughness of polycrystalline tungsten under mode I and mixed mode I/II loading. Mater Sci Eng A 1999;270:197–207.
[7] Tran-Huu-Loi, Morniroli JP, Gantois M, Lahaye M. Brittle fracture of polycrystalline tungsten. J Mater Sci 1985;20:199–206.